Climate patterns and phytoplankton dynamics in Antarctic latent heat polynyas

Martin A. Montes-Hugo[1] and Xiaojun Yuan[2]

Received 14 August 2010; revised 7 March 2012; accepted 5 April 2012; published 19 May 2012.

[1] Seasonal coherence between satellite-derived phytoplankton parameters (chlorophyll *a* concentration (Chl) and phytoplankton bloom initiation time (BIT)), environmental variables (sea ice concentration, surface solar radiation, and wind speed), and climate patterns (El Niño 3.4, the Southern Annular Mode, the Pacific South America pattern, the semiannual oscillation, and the wave-3 stationary pattern) was investigated in four latent heat polynyas (Amundsen Sea, western Ross Sea, Dumont d'Urville, and Prydz Bay) using data corresponding to 1998–2006 phytoplankton growing seasons. In general, polynyas in the western sector (i.e., Amundsen Sea and western Ross Sea) had a greater sea ice cover, lower solar radiation levels, higher and more variable Chl, and more variable and delayed (i.e., high BIT) phytoplankton blooms. Differences in Chl and BIT were mainly attributed to differences in water stratification and interannual variability of sea ice concentration caused by ice shelf calving events in the Ross Sea. Changes in solar radiation reaching the sea surface played an important role in determining phytoplankton blooms in the western Ross Sea and Prydz Bay. Stronger winds tend to benefit development of phytoplankton blooms in polynyas having more stratified waters. Sensitivity of phytoplankton to climate variability in polynyas under investigation was highly influenced by the polynya size during summer (e.g., Chl in Dumont d'Urville and BIT in the western Ross Sea). Also, the response of Chl to the same climate pattern changed with the polynya's location (e.g., correlation between Chl and El Niño 3.4 in Amundsen Sea (positive) and Dumont d'Urville (negative)).

Citation: Montes-Hugo, M. A., and X. Yuan (2012), Climate patterns and phytoplankton dynamics in Antarctic latent heat polynyas, *J. Geophys. Res.*, *117*, C05031, doi:10.1029/2010JC006597.

1. Introduction

[2] Coastal areas of the Antarctic Ocean with ice free waters during winter (polynyas) have an active role in modulating global climate variability due to their important influence on ocean uptake of atmospheric CO_2 [*Sweeney et al.*, 2000] and heat exchange [*Dare and Atkinson*, 2000] between the sea surface and lower tropospheric layers.

[3] Latent heat polynyas, the focus of this study, are mainly influenced by atmospheric forcing associated with katabatic winds [*Marshall and Turner*, 1997; *Adolphs and Wendler*, 1995], and concurrent transport of sea ice away from the coast [*Pease*, 1987].

[4] In general, phytoplankton abundance in latent heat polynyas is relatively high compared to the open ocean [*Arrigo et al.*, 1998]. Higher productivity is mainly related to a greater penetration of solar radiation in polynyas during spring and summer due to a lower cloudiness and a greater ice free surface area [*Arrigo and van Dijken*, 2003a].

[5] Coupling between phytoplankton dynamics and environmental variables in polynyas is linked to Antarctic climate patterns at interannual time scales. *Arrigo and van Dijken* [2003a] suggested a connection between size of polynya, a variable positively correlated with phytoplankton production, and anomalies of El Niño Southern Ocean Oscillation (ENSO). Also, they highlighted contrasting ice-atmosphere interactions according to the polynya location.

[6] The aim of this study is to expand our understanding of how large-scale climate variations in Antarctica modulate amplitude and timing of phytoplankton blooms developing in latent heat polynyas. The *Arrigo and van Dijken* [2003a] study on characterizing phytoplankton dynamics of 37 Antarctic polynyas is a valuable reference point for the current paper; however, this study didn't examine relationships between climate factors and phytoplankton variability.

[7] Here, we hypothesize that major Antarctic climate modes other than ENSO also have a substantial influence on

[1]Institut des Sciences de la Mer de Rimouski, Université du Québec à Rimouski, Rimouski, Québec, Canada.
[2]Lamont-Doherty Earth Observatory, Earth Institute at Columbia University, Palisades, New York, USA.

Corresponding author: M. A. Montes-Hugo, Institut des Sciences de la Mer de Rimouski, Université du Québec à Rimouski, 310 Alleé des Ursulines, Off. P-216, Rimouski, QC G5L 3A1, Canada. (martinalejandro_montes@uqar.ca)

0148-0227/12/2010JC006597

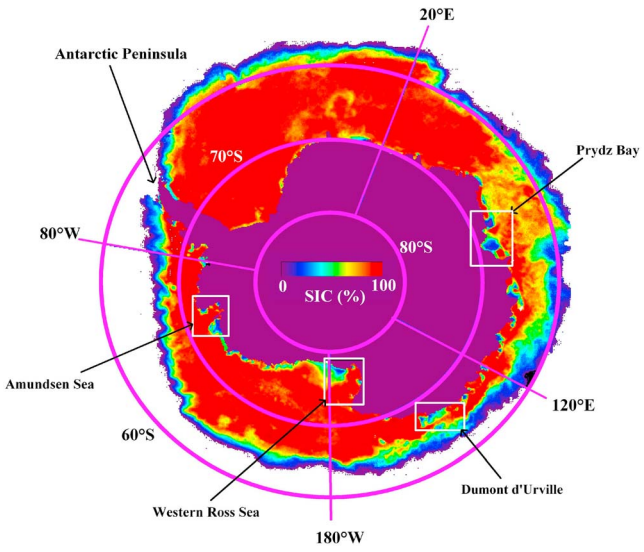

Figure 1. Geographic location of Antarctic latent heat coastal polynyas. A monthly composite of sea ice concentration during spring is used to indicate spatial boundaries of polynyas (white rectangles).

phytoplankton communities of latent heat polynyas during summer, as each polynya has a unique physical environment and location. Thus, each polynya is expected to have a specific response with respect to different climate modes.

[8] In the first part of this study, we quantified the relative importance of sea ice and surface solar radiation in determining summer phytoplankton blooms in four latent heat polynyas (Amundsen Sea, western Ross Sea, Dumont d'Urville, and Prydz Bay). In particular, we analyzed the effect of environmental variables on magnitude and timing of phytoplankton blooms as estimated from chlorophyll *a* concentration measured by satellites (Chl). In the second part, we studied relationships between seasonal anomalies of five climate patterns (El Niño 3.4 or EN3.4, Southern Annular Mode or SAM, Pacific South America pattern or PSA, semiannual oscillation or SAO, and wave-3 stationary pattern or W3) and phytoplankton bloom characteristics (magnitude and timing) at the seasonal scale. Mechanisms explaining relationships between Chl, environmental variables, and climate patterns are suggested. Also, instantaneous and delayed seasonal effects of environmental variables and climate modes on phytoplankton dynamics are examined and used to classify the polynyas under study.

2. Methods

2.1. Criteria for Selected Polynyas

[9] We chose three latent heat coastal polynyas, Amundsen Sea, western Ross Sea and Prydz Bay), based on their relative size (average surface area, summer: $>35 \times 10^3$ km^2, winter: $>3.5 \times 10^3$ km^2) [*Arrigo and van Dijken*, 2003a; *Kern*, 2009] (Figure 1). Also we selected an additional polynya (Dumont d'Urville) characterized by a relatively small size (open water area per year $<15 \times 10^3$ km^2), but having a long (30 year) time series of biological (e.g., penguin time series) and climate-related measurements [*Jenouvrier et al.*, 2003, 2005]. The geographic locations of latent heat polynyas under investigation are closely associated with major katabatic wind systems shown by the convergence of streamlines of cold air drainage off Antarctica [*Parish and Bromwich*, 1987]. Likewise, these locations are characterized by having strong air-sea heat fluxes, seasonal variations on sea ice and dense shelf water formation, and relatively high primary production rates [*Smith et al.*, 2000; *Arrigo and van Dijken*, 2003a; *Fusco et al.*, 2009].

2.2. Environmental Data Sets

2.2.1. Land-Based Meteorological Stations

[10] The weekly arithmetic average wind speed in m s^{-1} was obtained from in situ data obtained from automatic weather stations (available from University of Wisconsin, ftp://ice.ssec.wisc.edu/). These time series were located near the western Ross Sea (77.8°S, 166.7°E, McMurdo station), Dumont d'Urville (66.7°S, 140.0°E, Dumont d'Urville station) and Prydz Bay (70.9°S, 69.9°E, Amery Ice Shelf station) polynyas. The wind data are available since November 2004 in each polynya except Amundsen Sea, where no meteorological observations are available.

2.2.2. Satellite Measurements

[11] Chl values for each polynya were estimated using the NASA bio-optical model OC4V4 and SeaWiFS (Sea-viewing Wide Field-of-view Sensor) measurements of remote sensing reflectance corresponding to the visible–NIR spectral range. For all radiometric channels, satellite-based images were calibrated and geolocated at 4.5 km spatial resolution). Daily Chl data were browsed for each austral summer (i.e., December to February) of 1998–2007 years, and low-quality pixels were removed by using default NASA level 2 flags.

[12] For each polynya, phytoplankton bloom characteristics during each summer were characterized based on seasonal arithmetic average of Chl and phytoplankton bloom initiation time (BIT). The first metrics provides information about amplitude of phytoplankton blooms in surface waters (i.e., within the first optical depth or ~20 m in Antarctic coastal waters) [*Montes-Hugo et al.*, 2009, 2010]. The second metric relates to temporal lagging of the blooms during the season of maximum growth.

[13] Amplitude of phytoplankton blooms in the Southern Ocean is controlled by diverse factors (e.g., light, nutrients, viruses, zooplankton grazing) [*Lancelot et al.*, 2009]. Thus, Chl variation with time does not follow a monotonic increase, and is characterized instead by reaching a maximum followed in general by lower values toward the end of summer. For this reason, we included BIT as a time-dependent variable that is only related to the intrinsic growth of phytoplankton and factors limiting that specific growth.

[14] BIT is the week number (e.g., week 1 represents the first week of December) during summer when the weekly arithmetic average of Chl is 5% above the seasonal median [*Siegel et al.*, 2002]. This index is related more to bloom initiation than an index based on the time corresponding to the peak of chlorophyll *a* concentration [*Banse and English*, 1994]. Thus, BIT indicates the beginning of above normal Chl conditions or phytoplankton abundance levels above a certain background [*Longhurst*, 1998].

[15] Sea ice concentration (SIC) data were derived from microwave measurements (85 GHz) obtained with the Special Sensor Microwave Imager (SSMI) at a spatial

resolution of 12.5 km (Ifremer-CERSAT, Artist sea ice algorithm, NSIDC). This spatial resolution was enough to detect open water pixels even in latent heat polynyas having a relatively small size (i.e., Dumont d'Urville) during winter ($\sim < 1 \times 10^3$ km^2 or 6 SSMI pixels [*Arrigo and van Dijken*, 2003a, Table 1]). Images of sea ice concentration values ranging between 0 and 100% were browsed for winter (June–July–August), spring (September–October–November) and summer (December–January–February). Open water pixels were defined as those pixels having a sea ice concentration percentage below 10% [*Arrigo and van Dijken*, 2003a]. Land presence in each image was discriminated by using a high-resolution coastline (0.2 km) [*Wessel and Smith*, 1996]. Overall, retrieval uncertainty of satellite estimates of sea ice concentration varies between 2.5 and 10% [*Wiebe et al.*, 2009].

[16] Photosynthetically available radiation just above the sea surface (PAR(0+)) was estimated from satellite imagery (SeaWiFS, L3 level, footprint: 9 km, NASA). Similar to the satellite-based measurements of chlorophyll *a* and sea ice concentration, weekly image composites of solar radiation were created by calculating the arithmetic average of daily images. The overall uncertainty of monthly SeaWiFS-derived solar radiation in the photosynthetic spectrum, as derived from the sum of squared differences between measured and modeled values, is <10% [*Frouin et al.*, 2003].

2.3. Climates Indices

[17] In this study, we consider five climate modes that have distinct spatiotemporal characteristics and have recognizable influences on Antarctic sea ice [*Yuan and Li*, 2008; *Russell and McGregor*, 2010]. Although different mechanisms or processes generate these climate modes, their indices are not fully independent from each other. The time series of these climate modes are derived from or defined in the atmospheric variable in which they most prevail [*Yuan and Li*, 2008]. Together, they contribute to most of the climate variability of the Southern Ocean at interannual time scales.

[18] The Southern Annular Mode is defined by zonally symmetric but out-of-phase pressure anomalies between middle and high latitudes, and has influence over the whole Southern Hemisphere [*Gong and Wang*, 1999; *Thompson and Wallace*, 2000]. This index was calculated as the difference of normalized monthly zonal mean sea level pressure values estimated at 50°S and 65°S (NCEP/NCAR reanalysis data) [*Yuan and Li*, 2008].

[19] The semiannual oscillation describes another zonally symmetric mode in the southern extratropics, which is characterized by twice-yearly enhancement in meridional gradients of temperature and pressure fields [*Van Loon*, 1984; *Walland and Simmonds*, 1999]. The atmospheric convergence line with a strong half-year cycle exerts a significant influence on the seasonal advance/retreat of ice extent [*Enomoto and Ohmura*, 1990]. This index is generated by the differences of the zonal mean sea level pressure at 50°S and 65°S based on NCEP/NCAR reanalysis data [*Yuan and Li*, 2008].

[20] The quasi-stationary wave-3 pattern is a predominant winter mode in pressure/wind fields of the southern middle–high latitudes [*van Loon*, 1972; *Raphael*, 2004], actively interacting with the sea ice field at relatively low latitudes [*Raphael*, 2007; *Yuan and Li*, 2008]. Three southerly branches of this pattern coincide with three maxima of the northward extent of sea ice, indicating the role of this pattern in advancing the ice edge [*Yuan et al.*, 1999]. Time series for this climate pattern were constructed based on the leading empirical orthogonal function mode of surface meridional winds as computed from NCEP/NCAR reanalysis.

[21] The Pacific South America pattern is the counterpart of the Pacific North America pattern in the Northern Hemisphere, and represents an atmospheric wave train in the pressure field over the South Pacific and South America [*Karoly*, 1989]. It also represents a mechanism that propagates the ENSO signal from the tropics to the south forming the Antarctic Dipole [*Yuan*, 2004]. This climate pattern has a strong impact on sea ice fields of the western sector of Antarctic [*Yuan and Li*, 2008]. Similarly to the Pacific North American index, the Pacific South America index was obtained from NCEP/NCAR reanalysis and is defined by monthly 500 mb height anomalies at three anomalous height centers to the east of New Zealand, the Amundsen Sea and the Southwest Atlantic, respectively [*Yuan and Li*, 2008].

[22] El Niño 3.4 is defined based on sea surface temperature anomalies in the central tropical Pacific (120°W–170°W, 5°S–5°N) [*Reynolds et al.*, 2002]. Unlike the multivariate ENSO index [*Wolter and Timlin*, 1993], the El Niño 3.4 proxy is computed from NCEP/NCAR reanalysis data and does not include information about surface winds and cloud fraction.

2.4. Statistical Analysis

[23] Intensity of the relationship between seasonal anomalies of Chl during summer and environmental variables (sea ice and solar radiation) during the same season and preceding spring and winter of each year was calculated based on the magnitude of the nonparametric Spearman rank order correlation coefficient (ρ_S) [*Spearman*, 1904]. Due to the lack of temporal coverage, correlations between wind speed and Chl were conducted using monthly anomalies. Significant correlations were evaluated based on Student's *t* distribution test. The same statistical analysis was also applied to investigate degree of association between summer Chl and climate patterns during the preceding winter, spring and coincident summer conditions.

3. Results

[24] In this section, we investigate for each polynya (1) the interannual variability of phytoplankton parameters (i.e., Chl and BIT) during the maximum growing season, (2) the influence of sea ice, solar radiation, and wind intensity on phytoplankton development during late spring and summer at the seasonal scale, and (3) the linkage between phytoplankton dynamics and dominant climate patterns at interannual time scales.

3.1. Variability of Chlorophyll *a* Concentration in Polynyas

[25] In general, phytoplankton concentration, as inferred from Chl values, was higher and more variable in the Amundsen Sea and the western Ross Sea polynyas, two productive environments characterized by a relatively wide continental shelf [*Arrigo and van Dijken*, 2003a]. The largest range (0.16–7.76 mg m^{-3}) of weekly averaged Chl values

Table 1. Statistics of Satellite-Derived Phytoplankton Parameters and Environmental Variables[a]

		SIC		PAR(0+)		WS		Chl		BIT	
	Season	$\tilde{x}$	Range	$\tilde{x}$	Range	$\tilde{x}$	Range	$\tilde{x}$	Range	$\tilde{x}$	Range
AS	Winter	89.7	77.3–97.1								
	Spring	85.5	57.8–93.5								
	Summer	50.9	6.3–79.8	28.7	5.8–54.9			1.48	0.16–7.76	4.6	2–7
WRS	Winter	92.7	87.9–98.4			19.0	8–36				
	Spring	89.1	78.6–96.7			17.4	7–41				
	Summer	19.8	0.0–79.5	32.4	7.5–60.6	15.4	7–28	1.39	0.23–4.54	2.9	1–8
DU	Winter	88.2	81.8–95.4			20.9	10–42				
	Spring	79.2	60.3–95.5			20.4	9–48				
	Summer	33.1	15.5–65.6	34.6	15.5–59.7	18.4	11–30	0.52	0.18–3.09	3.0	1–5
PB	Winter	82.8	77.2–97.5			22.5	12–34				
	Spring	77.9	57.5–90.6			16.2	5–32				
	Summer	27.1	3.3–58.6	33.5	11.3–56.0	8.7	5–19	1.09	0.19–3.82	4.1	2–6

[a]Here $\tilde{x}$: seasonal arithmetic average, WS: wind speed in km h^{-1}, AS: Amundsen Sea, WRS: western Ross Sea, DU: Dumont d'Urville, and PB: Prydz Bay. SIC in %, PAR(0+) in mol quanta m^{-2} d^{-1}, Chl in mg m^{-3}, and BIT in weeks. Range is based on weekly values of arithmetic average ($\tilde{x}$). Acronyms Chl, SIC, and PAR(0+) are defined in section 2.

during summer were obtained in Amundsen Sea (Table 1). Conversely, polynyas located in East Antarctica had typically a smaller range of Chl values (0.18–3.09 mg m^{-3}).

[26] Phytoplankton bloom timing also differed between polynyas of the western sector (Amundsen Sea and western Ross Sea) and East Antarctica (Dumont d'Urville and Prydz Bay) polynyas. Indeed, BIT suggested that seasonal phytoplankton development was more variable between years and often delayed (initiation up to 8 weeks late) in those latent heat polynyas of the western sector (Table 1).

[27] The most dramatic changes on phytoplankton bloom initiation time between consecutive years were observed in the Ross Sea (e.g., phytoplankton growing seasons of 2001 and 2003, Figure 2). Likewise, the phytoplankton growth onset in the Ross Sea was clustered in two groups: either very early (week 1–2) or very late (week 6–8), which is likely caused by the presence of icebergs. In contrast, the BIT in the Amundsen Sea, Dumont d'Urville and Prydz Bay polynyas had relatively small year-to-year variations but the onset of phytoplankton growth was more or less evenly from 1 to 7 weeks (Figure 2).

3.2. Environmental Variability and Influence on Phytoplankton Blooms

[28] Sea ice cover during summer was negatively associated with averaged chlorophyll *a* concentration (e.g., Amundsen Sea, $\rho_S = -0.64$, t-Student = 2.33, $P = 0.047$; Dumont d'Urville, $\rho_S = -0.80$, t-Student = −3.85, $P = 0.005$) (Figure 3a). These regions presented persistent sea ice coverage (i.e., >25%) during summer (Table 1).

[29] Seasonal sea ice concentration was also an important factor modulating timing of phytoplankton blooms during each growing period (Figure 3b). Again, the most influenced polynyas were those presenting relatively high sea ice concentrations during summer (i.e., Amundsen Sea and Dumont d'Urville). However, the impact of sea ice conditions on the onset of phytoplankton bloom was delayed comparing to that related to changes on arithmetic averaged Chl concentrations.

[30] The solar radiation that reached the sea surface and was available for photosynthesis during summer in Dumont d'Urville was slightly higher (summer average up to 34.6 mol quanta m^{-2} d^{-1}) and less variable (maximum/minimum PAR(0+) up to 4) than other studied sites. Conversely, the Amundsen Sea polynya was characterized by cloudier skies (summer PAR(0+) average of 28.7 mol quanta m^{-2} d^{-1}) with more variable (5.8–54.9 mol quanta m^{-2} d^{-1}) sunlight conditions (Table 1).

[31] The western Ross Sea polynya was the only study area where variations of Chl during summer were substantially associated with solar radiation variations. This susceptibility was manifested in terms of Chl ($\rho_S = 0.627$, $P = 0.035$, Figure 4a) and BIT ($\rho_S = -0.778$, $P = 0.005$, Figure 4b). Also, surface illumination seemed to be an important factor determining phytoplankton pigments levels and timing of blooms in Prydz Bay waters, however these relationships were based on correlation results with a reduced statistical confidence (ρ_S (Chl-PAR(0+)) = 0.582, $P = 0.056$, ρ_S(BIT-PAR(0+)) = −0.365, $P = 0.275$).

[32] Based on correlation analysis, the effect of sea ice concentration and surface solar radiation on summer Chl was always negative and positive, respectively, in all polynyas under investigation (Figures 3a and 4a). However, this negative feedback was preferentially controlled by sea

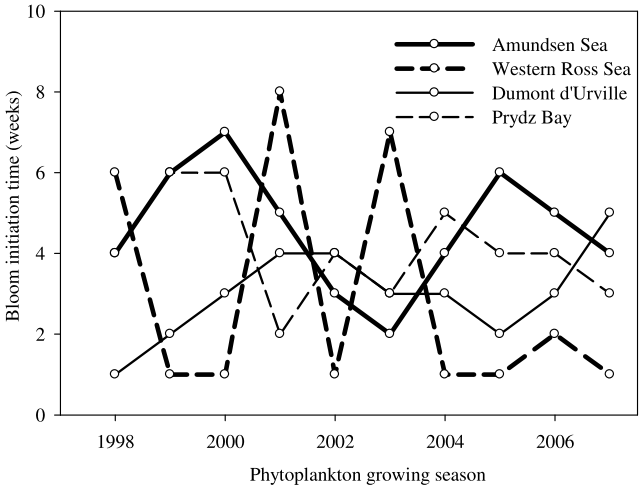

Figure 2. Interannual variability of phytoplankton bloom initiation time in latent heat polynyas.

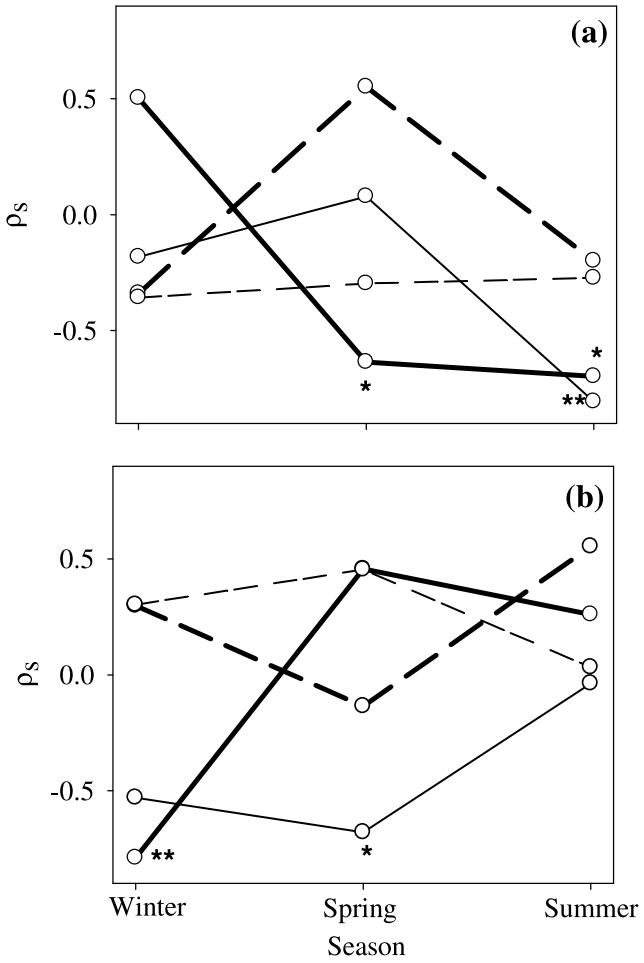

Figure 3. Relationships between satellite-derived chlorophyll *a* and sea ice concentration. (a) Spearman correlation between the arithmetic average of Chl summer anomalies and SIC anomalies (*y* axis) computed for the same period and previous spring and winter. (b) Same as Figure 3a, but calculations are based on BIT instead of Chl. Significant correlation at 95% (asterisk) and 99% (double asterisk) confidence levels is indicated. Symbols for each curve are described in Figure 2.

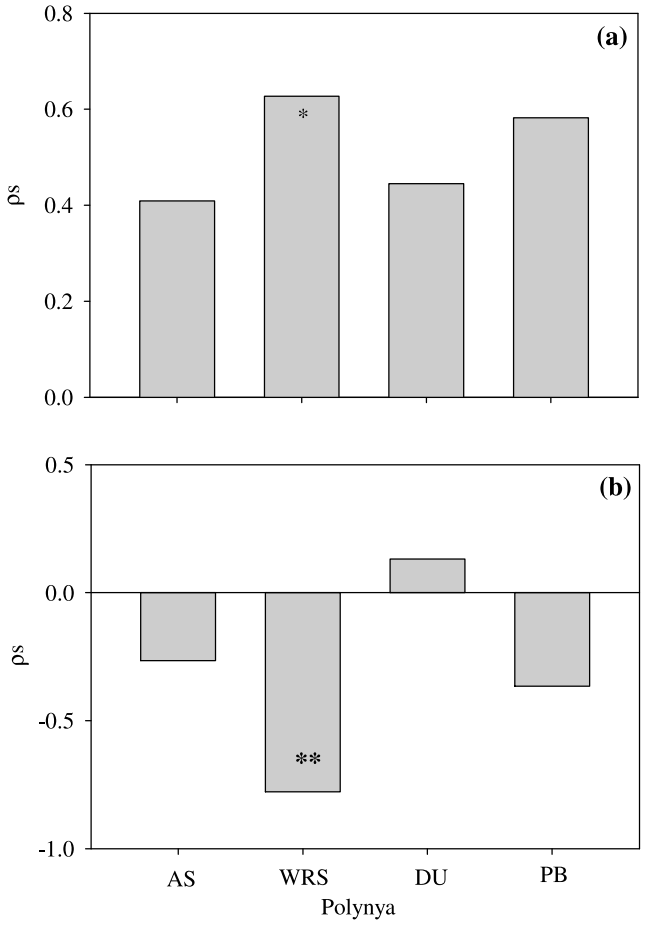

Figure 4. Response of satellite-derived phytoplankton parameters to solar radiation. AS: Amundsen Sea, WRS: western Ross Sea, DU: Dumont d'Urville, and PB: Prydz Bay. Each bar represents the Spearman correlation coefficient (*y* axis) between summer anomalies of PAR(0+) of (a) Chl or (b) BIT. Significant correlation at 95% (asterisk) and 99% (double asterisk) confidence levels is indicated.

ice in Amundsen Sea and Dumont d'Urville, and solar radiation in the western Ross Sea and Prydz Bay polynyas.

[33] A repetitive feature in all polynyas was the relaxation of wind intensity during the period of maximum phytoplankton growth (up to 61% from winter to summer in Prydz Bay, Table 1). Despite this common behavior, there was not a clear relationship between winter, spring or summer wind speed and summer phytoplankton concentration at the interannual scale. Further analysis of longer but coarser time series of wind data derived from satellites (e.g., QuickScat) will help to better understand relationships between wind speed and phytoplankton variability.

[34] Satellite-derived chlorophyll concentration during summer was directly or inversely related with wind speed depending on the polynya under investigation. In the western Ross Sea, Chl tended to increase during more windy conditions (ρ_S up to 0.527, P = 0.107, n = 10, spring), however an opposite scenario occurred in Prydz Bay and

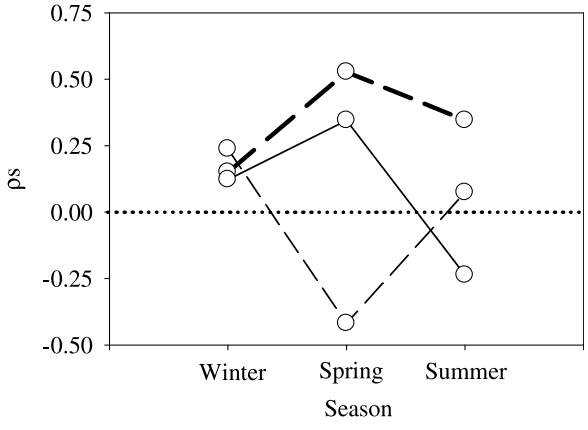

Figure 5. Correlation between satellite-derived chlorophyll *a* concentration and wind speed. Spearman correlation coefficient between monthly anomalies of wind speed and Chl (*y* axis). Zero correlation is depicted with a dotted line. Symbols for each curve are described in Figure 2.

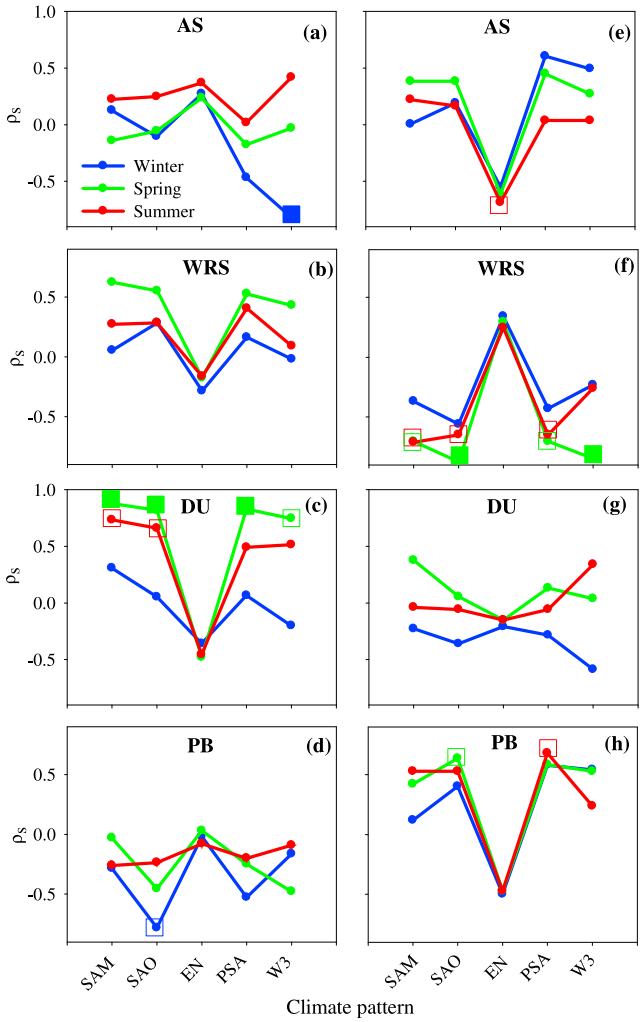

Figure 6. Relationships between satellite-derived parameters and climate patterns. Spearman correlation coefficient between seasonal anomalies of climate patterns (winter: blue, spring: green, and summer: red) and summer anomalies of (a–d) Chl or (e–h) BIT. Significant correlations at 95% (empty rectangle) and 99% (solid rectangle) confidence levels. Acronyms for polynyas and climate patterns (x axis) are defined in Figure 4 and in section 1.

Dumont d'Urville where development of phytoplankton blooms seem only favored during years characterized by calm days during spring and summer, respectively (ρ_S up to -0.419, $P = 0.213$, spring, Figure 5). Whether the above Chl responses to wind are also connected with changes on wind direction or be generalized to other polynyas is a topic that requires further investigation.

3.3. Climate Patterns and Seasonal Changes on Phytoplankton Blooms

[35] Response of phytoplankton to modes of climate during summer was highly influenced by the polynya size. Indeed, Chl in the polynya with the smallest surface area (Dumont d'Urville) was connected with a greater number of climate modes (up to 4, SAM, SAO, PSA and W3) with respect to those polynyas having a larger spatial dimensions (e.g., the western Ross Sea) (Figures 6a–6d). In addition, summer Chl in Dumont d'Urville polyna was more correlated with SAM, SAO, PSA and wave-3 in spring than in summer. The maximum correlation between summer Chl and spring SAM was up to 0.88 (t = 5.21, $P < 0.001$). The response of Chl in the western Ross Sea polynya to all climate modes was of the same sign as in Dumont d'Urville polyna but with lower correlation coefficients and less confidence levels (Figure 6b).

[36] In general for all polynyas investigated, the impact of winter climate anomalies on summer phytoplankton was weaker with respect to the effects of climate patterns on Chl occurring during spring or summer seasons. Some exceptions were found between winter wave-3 pattern and summer Chl in the Amundsen Sea polynya, and between winter SAO and summer Chl in the Prydz Bay polynya.

[37] Overall and based on correlation analysis, it is suggested that ENSO did not have a statistically significant impact on summer Chl concentration in any polynya under study, which is not surprising since our time series were rather short to resolve ENSO variability. However, persistency of ENSO signal throughout the year was coherent with the lack of seasonal variability on correlation coefficients between El Niño 3.4 index and summer Chl anomalies in each polynya.

[38] The Chl's response to ENSO variability was site-specific. During summer, correlation between Nino 3.4 index and Chl anomalies was positive in the Amundsen Sea polynya (ρ_S up to +0.37, t = 1.12, $P = 0.29$, summer) but negative in the Dumont d'Urville polynya (ρ_S up to -0.48, t = 1.54, $P = 0.16$, summer) (Figures 6a and 6c).

[39] Unlike Chl, timing of phytoplankton blooms in Dumont d'Urville polynya was not significantly correlated with variability on different climate patterns (Figure 6g). Conversely in the western Ross Sea, BIT was often correlated with spring and summer anomalies of all climate modes (ρ_S up to -0.65, t-Student = 2,41, $P = 0.04$) except for the Niño 3.4 index (Figure 6f).

[40] The strong coherence between BIT anomalies and El Niño 3.4 in the Amundsen Sea indicated the major influence of ENSO on phytoplankton communities of this Antarctic region (Figure 6e). This coupling was manifested during summer ($\rho_S = -0.69$, t-Student = 2.66, $P = 0.029$), and similar to Chl, was less variable between seasons with respect to that obtained using other climate indices.

4. Discussion

4.1. Environmental Regulation of Phytoplankton Blooms in Latent Heat Polynyas

[41] Our calculations of seasonal averages of Chl suggested an important longitudinal gradient in terms of pigment distributions between polynyas. Roughly, satellite measurements pointed out a clockwise increase of phytoplankton concentration with the highest values in the Amundsen Sea and the lowest values in East Antarctic polynyas. These spatial variations were associated with a maximum (minimum) of sea ice concentration and cloudiness in Amundsen Sea (Prydz Bay) polynyas. Thus, more light limitation of phytoplankton growth and synthesis of pigments are likely to occur in polynyas located toward the west to the western sector of the Antarctic coastline.

[42] The aforementioned spatial trends on sea ice and solar radiation are counterintuitive as massive phytoplankton blooms should be stimulated by a greater underwater illumination if other ecological factors are not limiting. This seems to be true for micronutrients such as iron [*Lancelot et al.*, 2009] but not for vertical mixing. Analysis of representative CTD profiles in each polynya (R. Sambrotto, personal communication, 2011) highlighted the importance of water stratification for explaining Chl patterns in Amundsen Sea and western Ross Sea with respect to Dumont d'Urville and Prydz Bay polynyas.

[43] An increase on stratification benefits phytoplankton development and accumulation of cells in the upper oceanic layers where light levels are more elevated. This phenomenon is modulated during spring and summer by the presence of sea ice cover. Relatively high sea ice concentration during summer was characteristic of Amundsen Sea and Dumont d'Urville polynyas, and was associated with negative correlations between Chl and SIC values. Likewise, the relatively low sea ice concentration during summer in western Ross Sea and Prydz Bay explains why Chl and PAR(0+) were substantially related in these two polynyas.

[44] Water stratification variations between polynyas was mainly attributed to salinity modifications caused by low-density water originated from melting of sea ice and snow cover, and freshwater fluxes derived from the continent related to disintegration of glaciers and ice shelves. This mechanism has been previously suggested by *Mitchell and Holm-Hansen* [1991] as an influence in other Antarctic marine ecosystems.

[45] Differences in wind-driven vertical mixing are unlikely to explain the spatial changes in water stratification between polynyas located between East Antarctic and the western sector. This is because polynyas located in East Antarctica had typically the strongest (seasonal average up to 13.3 m s^{-1} during spring, Dumont d'Urville) or weakest (up to 8.7 km h^{-1} during summer, Prydz Bay) winds during the period of maximum phytoplankton growth. Although land-based wind measurements are not available in Amundsen Sea, simulations of monthly wind fields during January 1980–1993 indicate comparable and relatively strong wind speeds (up to 32 m s^{-1}) between the Amundsen Sea and Dumont d'Urville polynyas [*van den Broeke and van Lipzig*, 2003].

[46] Timing of phytoplankton blooms tended to be more variable in those polynyas typically having greater sea ice concentrations throughout the year. In particular, the western Ross Sea was a special case where BIT had a large interannual variability between the summer of 2000 and 2004. What type of phenomena triggered such changes in timing of pigment fluctuations? Regionally speaking, the impact of sea ice on BIT was greater in a clockwise direction around the continent given the greater sea ice cover in the polynyas in the western sector of the coastline. In the Ross Sea the existence of massive icebergs may be the source of this variability. That was the case for phytoplankton growing seasons of 2001 and 2003, years that coincided with two major ice shelf calving events represented by the B-15 and the C-19 icebergs, respectively [*Arrigo et al.*, 2002; *Arrigo and van Dijken*, 2003b].

[47] The sporadic effect of large icebergs (i.e., >100 km long) is expected to cause anomalous late retreat of sea ice cover during spring and summer resulting in late development of phytoplankton blooms (i.e., higher BIT) due to a sharp reduction of underwater illumination, and lower nutrient supply linked to variability of coastal currents [*Smith et al.*, 2000; *Arrigo et al.*, 2002; *Arrigo and van Dijken*, 2003b]. Delayed BIT due to a reduction on water column illumination has also been reported in sea ice edge phytoplankton communities of East Antarctica [*Wright et al.*, 2010].

4.2. Response of Phytoplankton Communities to Local and Synoptic Variability of Climate Patterns

[48] Summer phytoplankton blooming characteristics in each polynya were associated with specific Antarctic climate mode patterns acting at various time scales (yearly to decadal) and with a different influence for each season. Variations of the Southern Annular Mode are mainly decadal and manifested on ocean-atmosphere circulation (annular component) and sea ice changes (nonannular component) [*Yuan and Li*, 2008; *Massom and Stammerjohn*, 2010]. Therefore is was not surprising to find no statistical significant ($P < 0.05$) relationships between the Southern Annular Mode anomalies and satellite-derived phytoplankton parameters for most of the comparisons made with the Spearman correlation coefficient.

[49] The summer amplitude and timing of the phytoplankton blooms in Amundsen Sea polynya was modulated by climate variations during the previous winter regime and linked to ENSO. What is the mechanism behind these correlations? According to *Yuan* [2004], a warm phase of ENSO (i.e., El Niño) is associated with negative sea ice anomalies in the vicinity of the Amundsen polynya. Therefore during El Niño conditions, the above correlations suggest a premature development of phytoplankton blooms (i.e., early BIT) and a large final yield of chlorophyll *a* during summer in the Amundsen Sea (Figures 2 and 6a–6e).

[50] The response of phytoplankton concentration, as inferred from Chl, to ENSO in Dumont d'Urville polynya contrasted with the one described for Amundsen Sea polynya. These differences (i.e., $+\rho_S$ in Amundsen Sea, $-\rho_S$ in Dumont d'Urville) are likely due to sea ice changes since ENSO events produce opposite sea ice anomalies in the Amundsen Sea and Dumont d'Urville region, as presented in *Yuan* [2004]. This supports the fact that the same climate pattern can have different effects on phytoplankton assemblages depending on the geographic location.

[51] At shorter time scales (<1 year) the semiannual oscillation is the most preponderant climate anomaly for driving surface temperature and wind patterns in Antarctica. In the Dumont d'Urville, the phytoplankton bloom initiation time showed a trend with the most recent phytoplankton blooms occurring later in the season (Figure 2). The delay in 2007 was probably associated with a greater sea ice extent during spring and early summer due to a decadal decrease on magnitude of semiannual oscillation pattern [*van den Broeke*, 2000].

[52] In summary, our results support the original hypothesis "Antarctic climate modes other than ENSO also have a major influence on phytoplankton variability of latent heat polynyas during summer, and this impact will vary between locations." Indeed, we showed that Antarctic climate modes not linked to ENSO (e.g., Southern Annular

Mode, semiannual oscillation) also played an important role in the defining amplitude and timing of phytoplankton blooms of specific polynyas (e.g., western Ross Sea and Dumont d'Urville). Likewise, this study supported the uniqueness of each polynya in terms of phytoplankton response to synoptic climate patterns for example opposite sign for the impact of ENSO events on the BIT in the western Ross Sea polynya versus the Amundsen Sea polynya.

[53] Although the results presented here provide clear indications that phytoplankton blooms in these coastal polynyas are responding to large climate variability in the Southern Ocean, the available time series are relatively short, preventing us deriving correlations with higher confidences. More studies are necessary to elucidate the effect of other oceanic factors (e.g., water stratification) linked to climate patterns and altering phytoplankton distribution between polynyas.

[54] **Acknowledgments.** This contribution was supported by NSERC discovery and CFI grants of Montes-Hugo, and NSF grants of ANT 07-39509 and ANT-1043669 for Yuan. Lamont contribution 7541.

References

Adolphs, U., and G. Wendler (1995), A pilot study on the interactions between katabatic winds and polynyas at the Adélie Coast, eastern Antarctica, *Antarct. Sci.*, *7*, 307–314, doi:10.1017/S0954102095000423.

Arrigo, K. R., and G. L. van Dijken (2003a), Phytoplankton dynamics within 37 Antarctic coastal polynya systems, *J. Geophys. Res.*, *108*(C8), 3271, doi:10.1029/2002JC001739.

Arrigo K. R., and G. L. van Dijken (2003b), Impact of iceberg C-19 on Ross Sea primary production, *Geophys. Res. Lett.*, *30*(16), 1836, doi:10.1029/2003GL017721.

Arrigo, K. R., D. Worthen, A. Schnell, and M. P. Lizotte (1998), Primary production in Southern Ocean waters, *J. Geophys. Res.*, *103*, 15,587–15,600, doi:10.1029/98JC00930.

Arrigo, K. R., G. L. van Dijken, D. G. Ainley, M. A. Fahnestock, and T. Markus (2002), Ecological impact of a large Antarctic iceberg, *Geophys. Res. Lett.*, *29*(7), 1104, doi:10.1029/2001GL014160.

Banse, K., and D. C. English (1994), Seasonality of coastal zone color scanner phytoplankton pigment in the offshore oceans, *J. Geophys. Res.*, *99*, 7323–7345, doi:10.1029/93JC02155.

Dare, R. A., and B. W. Atkinson (2000), Atmospheric response to spatial variations in concentration and size of polynyas in the Southern Ocean sea-ice zone, *Boundary Layer Meteorol.*, *94*, 65–88, doi:10.1023/A:1002442212593.

Enomoto, H., and A. Ohmura (1990), The influences of atmospheric half-yearly cycle on the sea ice extent in the Antarctic, *J. Geophys. Res.*, *95*, 9497–9511, doi:10.1029/JC095iC06p09497.

Frouin, R., B. A. Franz, and P. J. Werdell (2003), The SeaWiFS PAR product, in *Algorithm Updates for the Fourth SeaWiFS Data Reprocessing*, *SeaWiFS Postlaunch Tech. Rep. Ser.*, vol. 22, edited by S. B. Hooker and E. R. Firestone, pp. 46–50, NASA Goddard Space Flight Cent., Greenbelt, Md.

Fusco, G., G. Budillon, and G. Spezie (2009), Surface heat fluxes and thermohaline variability in the Ross Sea and in Terra Nova Bay polynya, *Cont. Shelf Res.*, *29*, 1887–1895, doi:10.1016/j.csr.2009.07.006.

Gong, D., and S. Wang (1999), Definition of Antarctic oscillation index, *Geophys. Res. Lett.*, *26*, 459–462, doi:10.1029/1999GL900003.

Jenouvrier, S., C. Barbraud, and H. Weimerskirch (2003), Effects of climate variability on the temporal population dynamics of southern fulmars, *J. Anim. Ecol.*, *72*, 576–587, doi:10.1046/j.1365-2656.2003.00727.x.

Jenouvrier, S., H. Weimerskirch, C. Barbraud, Y.-H. Park, and B. Cazelles (2005), Evidence of a shift in the cyclicity of Antarctic seabird dynamics linked to climate, *Proc. R. Soc. B*, *272*, 887–895, doi:10.1098/rspb.2004.2978.

Karoly, D. J. (1989), Southern Hemisphere circulation features associated with El Niño-Southern Oscillation events, *J. Clim.*, *2*, 1239–1252, doi:10.1175/1520-0442(1989)002<1239:SHCFAW>2.0.CO;2.

Kern, S. (2009), Wintertime Antarctic coastal polynya area: 1992–2008, *Geophys. Res. Lett.*, *36*, L14501, doi:10.1029/2009GL038062.

Lancelot, C., A. de Montety, H. Goosse, S. Becquevort, V. Schoemann, B. Pasquer, and M. Vancoppenolle (2009), Spatial distribution of the iron supply to phytoplankton in the Southern Ocean: A model study, *Biogeosciences*, *6*, 2861–2878, doi:10.5194/bg-6-2861-2009.

Longhurst, A. R. (1998), *Ecological Geography of the Sea*, Academic, San Diego, Calif.

Marshall, G. J., and J. Turner (1997), Katabatic wind propagation over the western Ross Sea observed using ERS-1 scatterometer data, *Antarct. Sci.*, *9*, 221–226, doi:10.1017/S0954102097000278.

Massom, R. A., and S. E. Stammerjohn (2010), Antarctic sea ice change and variability—Physical and ecological implications, *Polar Sci.*, *4*, 149–186, doi:10.1016/j.polar.2010.05.001.

Mitchell, B. G., and O. Holm-Hansen (1991), Observations of modeling of the Antarctic phytoplankton crop in relation to mixing depth, *Deep Sea Res., Part A*, *38*, 981–1007, doi:10.1016/0198-0149(91)90093-U.

Montes-Hugo, M., S. C. Doney, H. W. Ducklow, W. Fraser, D. Martinson, S. E. Stammerjohn, and O. Schofield (2009), Recent changes in phytoplankton communities associated with rapid regional climate change along the western Antarctic Peninsula, *Science*, *323*, 1470–1473, doi:10.1126/science.1164533.

Montes-Hugo, M., C. Sweeney, S. C. Doney, H. Ducklow, R. Frouin, D. G. Martinson, S. Stammerjohn, and O. Schofield (2010), Seasonal forcing of summer dissolved inorganic carbon and chlorophyll *a* on the western shelf of the Antarctic Peninsula, *J. Geophys. Res.*, *115*, C03024, doi:10.1029/2009JC005267.

Parish, T. R., and D. H. Bromwich (1987), The surface windfield over the Antarctic ice sheets, *Nature*, *328*, 51–54, doi:10.1038/328051a0.

Pease, C. H. (1987), The size of wind-driven coastal polynyas, *J. Geophys. Res.*, *92*, 7049–7059, doi:10.1029/JC092iC07p07049.

Raphael, M. N. (2004), A zonal wave 3 index for the Southern Hemisphere, *Geophys. Res. Lett.*, *31*, L23212, doi:10.1029/2004GL020365.

Raphael, M. N. (2007), The influence of atmospheric zonal wave three on Antarctic sea ice variability, *J. Geophys. Res.*, *112*, D12112, doi:10.1029/2006JD007852.

Reynolds, R. W., N. A. Rayner, T. M. Smith, D. C. Stokes, and W. Wang (2002), An improved in situ and satellite SST analysis for climate, *J. Clim.*, *15*, 1609–1625, doi:10.1175/1520-0442(2002)015<1609:AIISAS>2.0.CO;2.

Russell, A., and G. R. McGregor (2010), Southern Hemisphere atmospheric circulation: Impacts on Antarctic climate and reconstructions from Antarctic ice core data, *Clim. Change*, *99*, 155–192, doi:10.1007/s10584-009-9673-4.

Siegel, D. A., S. C. Doney, and J. A. Yoder (2002), The North Atlantic spring phytoplankton bloom and Sverdrup's critical depth hypothesis, *Science*, *296*, 730–733, doi:10.1126/science.1069174.

Smith, W. O., Jr., J. Marra, M. R. Hiscock, and R. T. Barber (2000), The seasonal cycle of phytoplankton biomass and primary productivity in the Ross Sea, Antarctica, *Deep Sea Res., Part II*, *47*, 3119–3140, doi:10.1016/S0967-0645(00)00061-8.

Spearman, C. (1904), The proof and measurement of association between two things, *Am. J. Psychol.*, *15*, 72–101, doi:10.2307/1412159.

Sweeney, C., et al. (2000), Nutrient and carbon removal ratios and fluxes in the Ross Sea, Antarctica, *Deep Sea Res., Part II*, *47*, 3395–3421, doi:10.1016/S0967-0645(00)00073-4.

Thompson, D. W. J., and J. M. Wallace (2000), Annular modes in the extratropical circulation. Part I: Month-to-month variability, *J. Clim.*, *13*, 1000–1016, doi:10.1175/1520-0442(2000)013<1000:AMITEC>2.0.CO;2.

van den Broeke, M. R. (2000), On the interpretation of Antarctic temperature trends, *J. Clim.*, *13*, 3885–3889, doi:10.1175/1520-0442(2000)013<3885:OTIOAT>2.0.CO;2.

van den Broeke, M. R., and N. P. M. van Lipzig (2003), Factors controlling the near-surface wind field in Antarctica, *Mon. Weather Rev.*, *131*, 733–743, doi:10.1175/1520-0493(2003)131<0733:FCTNSW>2.0.CO;2.

van Loon, H. (1972), Pressure in the Southern Hemisphere, in *Meteorology of the Southern Hemisphere*, *Meteorol. Monogr.*, vol. 13, edited by C. W. Newton, pp. 59–86, Am. Meteorol. Soc., Boston.

Van Loon, H. (1984), The Southern Oscillation. Part III: Associations with the trades and with the trough in the westerlies of the South Pacific Ocean, *Mon. Weather Rev.*, *112*, 947–954, doi:10.1175/1520-0493(1984)112<0947:TSOPIA>2.0.CO;2.

Walland, D., and I. Simmonds (1999), Baroclinicity, meridional temperature gradients, and the southern semiannual oscillation, *J. Clim.*, *12*, 3376–3382, doi:10.1175/1520-0442(1999)012<3376:BMTGAT>2.0.CO;2.

Wessel, P., and W. H. F. Smith (1996), A global, self-consistent, hierarchical, high-resolution shoreline database, *J. Geophys. Res.*, *101*, 8741–8743, doi:10.1029/96JB00104.

Wiebe, H., G. Heygster, and T. Markus (2009), Comparison of the ASI ice concentration algorithm with Landsat-7 ETM+ and SAR imagery, *IEEE Trans. Geosci. Remote Sens.*, *47*, 3008–3015, doi:10.1109/TGRS.2009.2026367.

Wolter, K., and M. S. Timlin (1993), Monitoring ENSO in COADS with a seasonally adjusted principal component index, paper presented at 17th Climate Diagnostics Workshop, Okla. Clim. Surv., Norman.

Wright, S. W., R. L. van den Enden, I. Pearce, A. T. Davidson, F. J. Scott, and K. J. Westwood (2010), Phytoplankton community structure and stocks in the Southern Ocean (30–80°E) determined by CHEMTAX analysis of HPLC pigment signatures, *Deep Sea Res., Part II*, *57*, 758–778, doi:10.1016/j.dsr2.2009.06.015.

Yuan, X. (2004), ENSO-related impacts on Antarctic sea ice: A synthesis of phenomenon and mechanisms, *Antarct. Sci.*, *16*, 415–425, doi:10.1017/S0954102004002238.

Yuan, X., and C. Li (2008), Climate modes in southern high latitudes and their impacts on Antarctic sea ice, *J. Geophys. Res.*, *113*, C06S91, doi:10.1029/2006JC004067.

Yuan, X., D. G. Martinson, and W. T. Liu (1999), Effect of air-sea-ice interaction on winter 1996 Southern Ocean subpolar storm distribution, *J. Geophys. Res.*, *104*, 1991–2007, doi:10.1029/98JD02719.